10.1

SIMPLE NUMERICAL SIMULATIONS OF CONVECTIVE LINES WITH LEADING STRATIFORM PRECIPITATION

Matthew D. Parker* and Richard H. Johnson
Colorado State University, Fort Collins, Colorado

1. INTRODUCTION

In investigating linear mesoscale convective systems (MCSs) of the central United States, Parker and Johnson (2000; hereafter PJ00) found that a common mode of MCS organization comprises a convective line with leading stratiform precipitation (hereafter called an LS MCS). Although PJ00 showed that some LS MCSs are sustained by rear inflow (for more information see Pettet and Johnson 2001), the LS systems that they studied experienced, on average, front–to–rear lower tropospheric winds (i.e., the MCSs were *front–fed*). This mean structure implies that, for some LS MCSs, inflow must pass through a region of pre–line precipitation before entering the convective towers.

We are currently performing idealized numerical simulations of front–fed LS MCSs. From our prior and ongoing work, we wish to discover: *1)* whether an idealized front–fed LS MCS can be long–lived in a numerical model, *2)* whether long–lived front–fed LS MCSs can be simulated in two dimensions (2–D), *3)* mesoscale flow fields that are consistent with both the observations of PJ00 and simulated front–fed LS MCSs, and *4)* to what environmental fields simulated front–fed LS MCSs are most sensitive. In this paper, we present results from some preliminary work in which we simulated LS MCSs in 2–D, and we elaborate on a possible quasi–stable structure for them.

2. MODEL CONFIGURATION

For our ongoing studies, we are using the Advanced Regional Prediction System (ARPS), version 4.5.0. The fundamental formulation of the ARPS was presented by Xue et al. (1995). For the simulations described herein, we used a 6–category ice microphysics scheme, open lateral boundary conditions, a $1\frac{1}{2}$–order TKE–based sub–gridscale closure, and a free–slip lower boundary. We neglected the effects of radiation and Coriolis accelerations. In our 2–D simulations, we used a grid that was 600 km long and 18.3 km deep, with a horizontal grid spacing of 1 km and a stretched vertical grid whose spacing ranged from 250 m near the surface to 730 m in the stratosphere. Although we don't discuss their details in this paper, we have also conducted some preliminary three–dimensional (3–D) simulations on smaller, coarser grids.

Each simulation's initial condition was horizontally homogeneous. We initiated convection during our simulations by adding to the initial states a cold pool that was 2 km deep and represented a uniform temperature perturbation of -3.2 K (the smallest magnitude that would initiate long–lived convection), and whose leading edge was centered in the model domain.

3. INITIAL BASE STATE SOUNDING

We averaged 59 *warm sector* soundings from PJ00 along with 30 soundings for *classifiable* systems from Houze et al. (1990, as inferred from their Fig. 15). We prescribed a 1 km deep mixed layer with constant potential temperature (θ) and vapor mixing ratio (q_v) for the

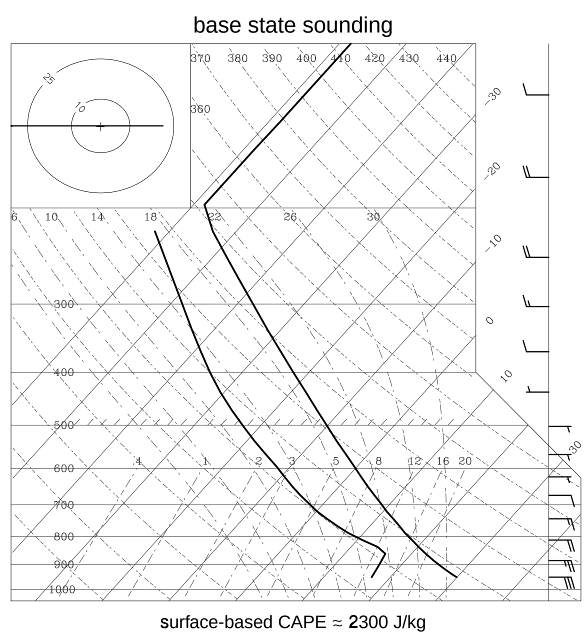

Figure 1: Skew–*T* ln–*p* and hodograph plots of the base state sounding and wind profile for this modeling study. Wind barb=5 m s^{-1}, half barb=2.5 m s^{-1}.

Corresponding author address: Matthew D. Parker, Department of Atmospheric Science, Colorado State University, Fort Collins, CO 80523-1371; E-mail: parker@squall.atmos.colostate.edu

sounding, assigning to it the maximal values of θ and q_v from the sounding's lowest 1 km. Then, we constructed analytic functions that very closely approximate the temperature and humidity profiles of the mean MCS sounding. What resulted, as shown in Fig. 1, was slightly smoothed but is nevertheless representative of the mean environment for midlatitude linear MCSs. In order to derive a wind profile for our simulations of LS MCSs (see Fig. 1), we averaged proximate NOAA wind profiler data for four archetypal LS systems from the population studied by PJ00, adding a constant (determined via trial and error) to keep the simulated systems centered within the domain. As of this writing, we have only considered the line–normal component of the flow. Given the low–level westerly shear, we expected convection to develop on the cold pool's east side, with the westerly storm–relative flow aloft contributing to an LS structure, as suggested by PJ00.

4. BASIC SIMULATION RESULTS

Even though a 3–D simulation using the base sounding in Fig. 1 (hereafter BASE) produced a long–lived, front–fed LS convective system, our 2–D BASE simulation did not. Although we don't discuss in this paper the detailed reasons for this failure, it appears to have occurred because gravity waves decelerated the lower tropospheric inflow. In both the 3–D BASE simulation (wherein gravity waves radiated both zonally and meridionally), and in 2–D simulations with less CAPE (description follows), the effects of such gravity waves were weaker, and long–lived systems resulted.

In attempting to simulate a long–lived 2–D LS system, we decreased the BASE sounding's surface temperature by 2 K while preserving its temperature at the tropopause and the general shape of its temperature profile; we also did not alter the BASE specific humidity profile. Hereafter, we refer to this modified sounding as BASE–2K. The BASE–2K sounding had less surface–based CAPE and more CIN than the BASE sounding. As a result, the simulated 2–D convective system avoided the failure mode mentioned above, and produced a long–lived MCS that exhibited an LS structure for some time.

After 35 min of the BASE–2K simulation, the initially forced convection had produced its own surface cold outflow, whose temperature perturbation was more than twice that of the initial cold pool trigger. Thereafter, new convective cells developed along the leading edge of the convectively generated cold pool. From about 45 min through 260 min of simulated time, the BASE–2K system exhibited a *quasi–stable* period, in which it had a front–fed LS structure and generated new convective cells periodically (Fig. 2), and in which the general character of the mesoscale flow field did not change.

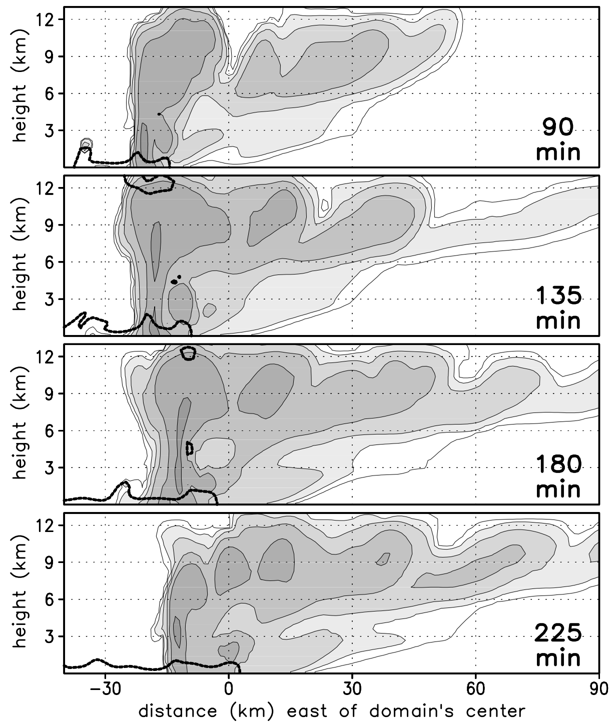

Figure 2: Total hydrometeor mixing ratio (q_h) and cold pool location for selected times during the BASE–2K LS system's quasi–stable period; q_h thinly contoured and shaded at 0.005, 0.02, 0.08, 0.32, 1.28, and 5.12 g kg^{-1}; general cold pool position indicated by $\theta' =$ –4 K isopleths (thick contours).

Later, as the cold low–level outflow surged ahead of the convective line's quasi–stable location, the line propagated eastward. This decreased the westerly component of the storm–relative winds aloft, thereby producing a structure that decreasingly resembled the LS mode and increasingly resembled the TS mode. Although we have not yet analyzed the process by which the simulated systems' cold pools overwhelmed the opposing low–level winds and low–level shear, this behavior occurred in most of our simulations, a modeling result that is consistent with PJ00's observation that some LS MCSs evolve toward TS structure.

5. A QUASI-STABLE LS STRUCTURE

In our preliminary 3–D simulations, we found that the flow fields for front–fed LS systems were non–trivially three dimensional. However, the 3–D simulations produced long–lived front–fed LS systems whose temporally–averaged along–line mean fields were very similar to those of our 2–D BASE–2K simulation (Fig. 3).

During its quasi–stable period, the BASE–2K system exhibited a fairly narrow, erect, deep convective line, whose associated stratiform precipitation fell almost

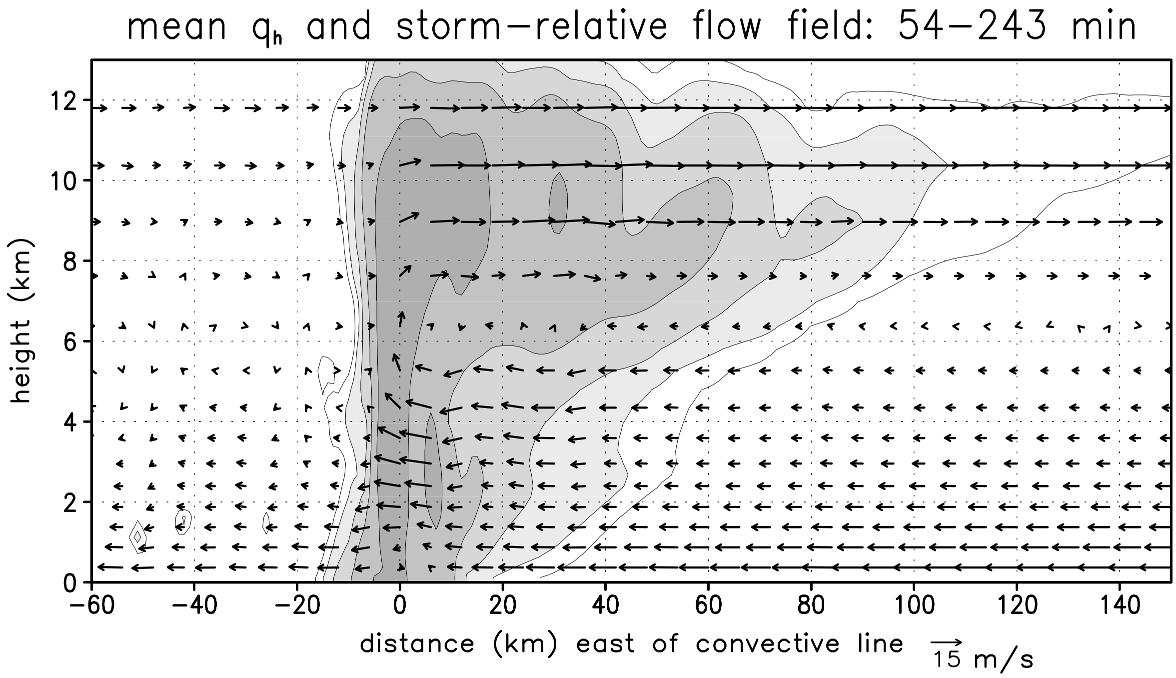

Figure 3: Temporally averaged total hydrometeor mixing ratio (q_h) and 2–D storm–relative flow during the BASE–2K LS system's quasi–stable period; q_h depicted as in Fig. 2; wind vectors (m s^{-1}) scaled as shown bottom right.

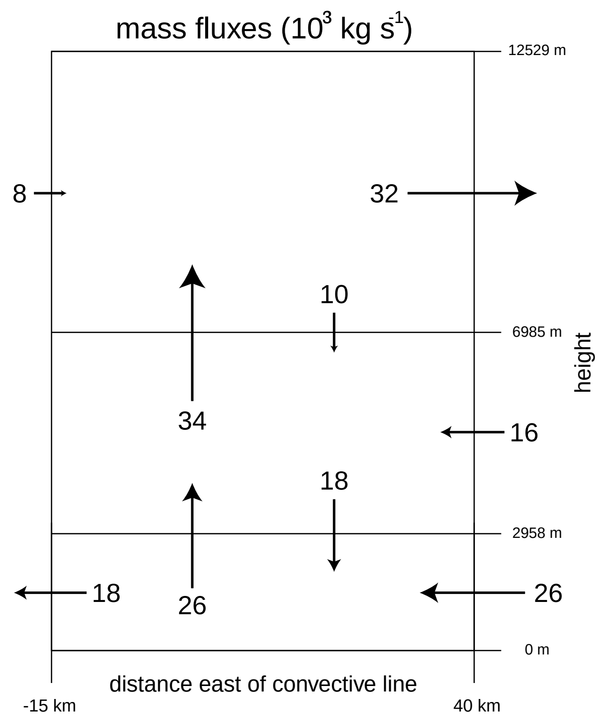

Figure 4: Temporally averaged (over the period from 54–243 min) mass fluxes (kg s^{-1}) through a region containing the convective line of the BASE–2K simulation. The values are obtained for an x–z slab that is 1 m wide.

entirely on the line's inflow side. In this regard, it apparently corresponds with the front–fed LS systems observed by PJ00. In addition, both the simulated line–leading and line–trailing wind profiles correspond remarkably well with our observations for LS systems from the central U.S., including those presented by PJ00.

In our analysis of mass fluxes (Fig. 4) and trajectories (Fig. 5), it became clear that there were four predominant flow branches in the simulated front–fed LS systems. Lower tropospheric inflowing air generally either ascended in the main overturning updraft (traj. A–a in Fig. 5), or followed an *up–down* trajectory and entered the system's cold pool (trajs. B–b and C–c). Some of the up–down parcels were left in the system's wake and advected away (traj. C–c), while others became part of the cold pool's nose (traj. B–b), occasionally recirculating several times in a rotor (e.g., at $z < 1$ km, $x = +5$ km in Fig. 3). The cold pool was also fed by mid–level parcels which descended in rainy downdrafts (traj. D–d in Fig. 5). Some mid–level front–to–rear flowing parcels also entered the main updraft (traj. E–e).

As parcels approached the convective line and passed through the pre–line precipitation, their θ_e was approximately conserved (θ_e in Fig. 6). The lower–θ_e parcels above the mixed layer (e.g. C-c, D-d, E-e) were chilled by as much as 2 K owing to evaporation, melting, and sublimation (θ_v' in Fig. 6). However, the low–level parcels (e.g. A-a) were chilled comparatively little in the pre–line precipitation region (θ_v' in Fig. 6), probably

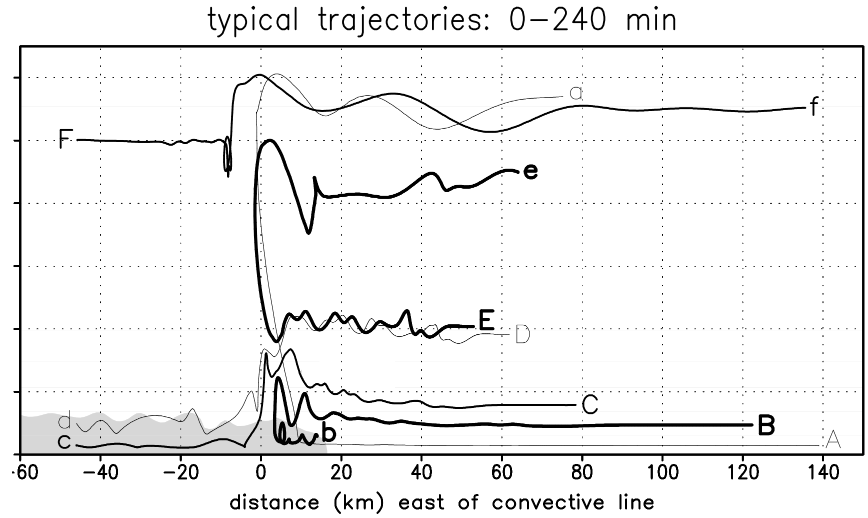

Figure 5: Four–hour parcel trajectories typifying commonly observed airstreams for BASE–2K simulation. Parcels' initial positions (at $t = 0$ min) are indicated by capital letters. Parcels' final positions (at $t = 240$ min) are indicated by lower–case letters. Averaged $\theta' < -2$ K are shaded to indicate the mean position of the surface cold pool during the time period. The trajectories' thicknesses vary in order to assist in differentiating them. The thicknesses have no additional meaning.

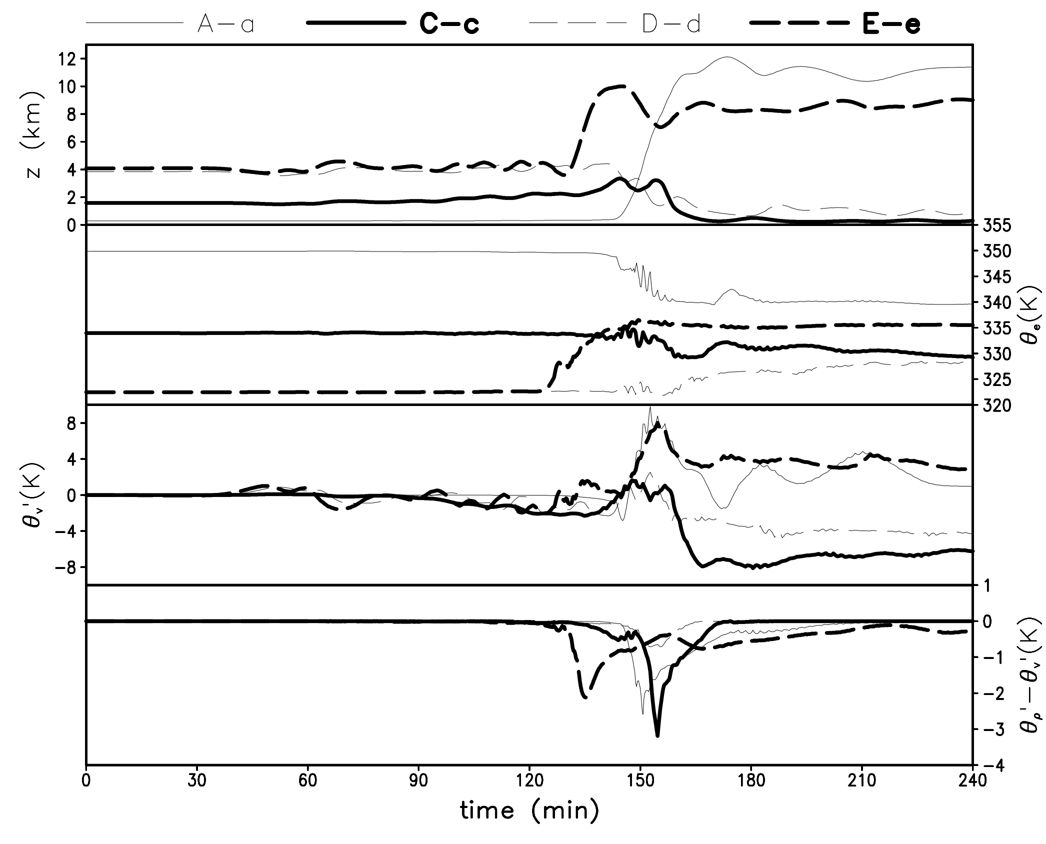

Figure 6: Height and thermodynamic properties along selected parcel trajectories from Fig. 5. From top to bottom, the panels depict: height above ground (z, km); equivalent potential temperature (θ_e, K); perturbation virtual potential temperature (θ'_v, K); and difference between perturbation density potential temperature and perturbation virtual potential temperature ($\theta'_\rho - \theta'_v$, K). $\theta'_\rho - \theta'_v$ expresses—in terms of a temperature perturbation—the contribution to buoyancy by hydrometeor loading. To infer a parcel's horizontal position, compare its height to the trajectories in Fig. 5.

because of the smaller hydrometeor mixing ratios near the surface in our simulations.

Both the cold pool's and updraft's θ_e generally represented a mixture of the high–θ_e lower tropospheric, and low–θ_e middle tropospheric, air parcels. Certain mixtures of low and mid–level air were potentially buoyant (i.e. had CAPE) and were able to ascend in the updraft despite their initially negative buoyancies (e.g. parcels A-a and E-e, Figs. 5 and 6). Pre–line precipitation was not detrimental to the long–lived system because the gust front lifted the cooled inflowing parcels to their levels of free convection. Other mixtures of low and mid–level air were not potentially buoyant, and eventually fed the surface cold pool (e.g. parcels C-c and D-d, Figs. 5 and 6). Most of the downdraft parcels' initial descents were due to hydrometeor loading (cf. θ_v' and $\theta_\rho' - \theta_v'$ in Fig. 6), although the contribution to negative buoyancy by temperature eventually overwhelmed the contribution by hydrometeor loading.

As seen in Fig. 3, the upper tropospheric flow west of the 2–D system was comparatively stagnant, although some parcels (traj. F–f in Fig. 5) did mix with the cloud and become entrained into the main overturning updraft. The general magnitudes of the airstreams represented in Fig. 5 are evident in the convective region's temporally–averaged 2–D mass fluxes (Fig. 4). The predominant flow branch was an overturning updraft, fed mostly by low–level inflow, but also by mid–level air. Front–to–rear flow was also important in that it helped to maintain the system–scale cold pool, which expanded rearward away from the convective line.

As described earlier in this section, a great deal of interaction happened between the lower and middle tropospheric inflow, and buoyancy sorting of the various mixtures of lower and middle tropospheric air apparently determined the relative magnitudes of the updraft and downdraft mass fluxes. Notably, much as described by Fovell and Tan (1998), the BASE–2K convection was periodically promoted (and alternately supressed) every 10–15 min during the quasi–stable period of the simulation, such that the upward and downward airstreams periodically increased and decreased in their prevalence and in the magnitudes of their mass fluxes.

6. CONCLUDING REMARKS

Based upon our atmospheric data and the idealized numerical simulations summarized above, a dynamically consistent conceptual model for front–fed LS MCSs is emerging. The ARPS was able to simulate such systems in 2–D; the 2–D simulations are of independent interest, and also help us to anticipate and explain the gross characteristics of our ongoing 3–D modeling work. Foremost among our preliminary conclusions are the following.

Simulated front–fed LS systems can be quasi–stable on timescales of hours. The flow structure for these quasi–stable simulated systems matches well with environmental data. It comprised a predominant overturning updraft, fed mostly by flow from the line–leading side in the lower troposphere, but also by entrained middle tropospheric air. Both lower tropospheric parcels and middle tropospheric parcels (which descended and crossed over the updraft's mean position) also contributed to the systems' surface cold pools. The middle and upper tropospheric flow to the systems' west was relatively stagnant. Inflowing lower and middle tropospheric parcels were moistened and chilled as they traversed the pre–line precipitation region; it appears that mixing and buoyancy sorting then determined whether they fed the system's updrafts or downdrafts. Provided that strong lifting occurred at the gust front, the cooling of inflow parcels in the LS region did not appear to be a detriment to the simulated long–lived systems.

In our continuing work, we are beginning to use more powerful computers in order to perform more highly resolved 3–D simulations on larger grids. We are also attempting to procure better atmospheric data for comparison to, and verification of, our idealized simulations. Finally, we are attempting to understand simulated LS systems' sensitivity to their environments' wind and thermodynamic profiles, and to understand the importance of storm–scale and system–scale processes to the systems' longevity.

ACKNOWLEDGMENTS

The National Science Foundation funded this research under grant ATM–0071371.

REFERENCES

Fovell, R.G., and P.–H. Tan, 1998: The temporal behavior of numerically simulated multicell–type storms. Part II: The convective cell life cycle and cell regeneration. *Mon. Wea. Rev.*, **126**, 551–577.

Houze, R.A., Jr., B.F. Smull, and P. Dodge, 1990: Mesoscale organization of springtime rainstorms in Oklahoma. *Mon. Wea. Rev.*, **118**, 613–654.

Pandya, R.E., and D.R. Durran, 1996: The influence of convectively generated thermal forcing on the mesoscale circulation around squall lines. *J. Atmos. Sci.*, **53**, 2924–2951.

Parker, M.D., and R.H. Johnson, 2000: Organizational modes of midlatitude mesoscale convective systems. *Mon. Wea. Rev.*, **128**, 3413–3436.

Pettet, C.R., and R.H. Johnson, 2001: Vertical structure and characteristics of two leading stratiform mesoscale convective systems. Preprints, *Ninth Conf. Mesoscale Processes*, Fort Lauderdale, FL, Amer. Meteor. Soc., elsewhere in this volume.

Xue, M., K.K. Droegemeier, V. Wong, A. Shapiro, and K. Brewster, 1995: ARPS version 4.0 user's guide. 380 pp. [Available from Center for Analysis and Prediction of Storms, University of Oklahoma, Norman, OK 73019-1011.]